Complementary evolution of coding and noncoding sequence underlies mammalian hairlessness

Amanda Kowalczyk, Maria Chikina, Nathan Clark

Abstract

Body hair is a defining mammalian characteristic, but several mammals, such as whales, naked mole-rats, and humans, have notably less hair than others. To find the genetic basis of reduced hair quantity, we used our evolutionary-rates-based method, RERconverge, to identify coding and noncoding sequences that evolve at significantly different rates in so-called hairless mammals compared to hairy mammals. Using RERconverge, we performed an unbiased, genome-wide scan over 62 mammal species using 19,149 genes and 343,598 conserved noncoding regions to find genetic elements that evolve at significantly different rates in hairless mammals compared to hairy mammals. We show that these rate shifts resulted from relaxation of evolutionary constraint on hair-related sequences in hairless species. In addition to detecting known and potential novel hair-related genes, we also discovered hundreds of putative hair-related regulatory elements. Computational investigation revealed that genes and their associated noncoding regions show different evolutionary patterns and influence different aspects of hair growth and development. Many genes under accelerated evolution are associated with the structure of the hair shaft itself, while evolutionary rate shifts in noncoding regions also included the dermal papilla and matrix regions of the hair follicle that contribute to hair growth and cycling. Genes that were top-ranked for coding sequence acceleration included known hair and skin genes *KRT2*, *KRT35*, *PKP1*, and *PTPRM* that surprisingly showed no signals of evolutionary rate shifts in nearby noncoding regions. Conversely, accelerated noncoding regions are most strongly enriched near regulatory hair-related genes and microRNAs, such as *mir205*, *ELF3*, and *FOXC1*, that themselves do not show rate shifts in their protein-coding sequences. Such dichotomy highlights the interplay between the evolution of protein sequence and regulatory sequence to contribute to the emergence of a convergent phenotype.

Introduction

Hair is a defining mammalian characteristic with a variety of functions, from sensory perception to heat retention to skin protection (Pough, Heiser, & McFarland, 1989). Although the mammalian ancestor is believed to have had hair, and in fact the development of hair is a key evolutionary innovation along the mammalian lineage (Eckhart et al., 2008), numerous mammals subsequently lost much of their hair. Many marine mammals, including whales, dolphins, porpoises, manatees, dugongs, and walruses, have sparse hair coverage likely related to hydrodynamic adaptations to allow those species to thrive in a marine environment (Z. Chen, Wang, Xu, Zhou, & Yang, 2013; Nery, Arroyo, & Opazo, 2014). Large terrestrial mammals such as elephants, rhinoceroses, and hippopotamuses also have little hair, likely to enable heat dissipation diminished by the species' large sizes (Fuller, Mitchell, Maloney, & Hetem, 2016). Notably, humans are also relatively hairless, a phenotypic characteristic that, while stark, has long been of mysterious origin (Kushlan, 1980). Just as hair coverage varies across mammal species, coverage for an individual organism can change over time in response to environmental factors. For example, Arctic mammals such as foxes and hares famously demonstrate dramatic coat changes in different seasons (Johnson, 1981).

Hair follicles are established during embryonic development as a result of interactions between epithelial and mesenchymal cells in the skin, and such interactions also drive follicle

movement in adults (Zhou et al., 2018). Hair follicles consist of a complex set of structures under the skin that support the hair shaft itself, which protrudes above the skin. The hair shaft contains an outer layer called the cuticle, an inner cortex later, and sometimes a central medulla core (Plowman, Harland, & Deb-Choudhury, 2018). Structures under the skin support the growth and formation of the hair follicle. Of particular interest are the dermal papilla and matrix region, both located at the base of the hair follicle. The dermal papilla is a key controller of regulation of hair growth and follicle morphogenesis (Veraitch et al., 2017). In fact, transplantation of dermal papilla cells has been repeatedly demonstrated to result in hair growth in previously hairless tissue (C. A.B. Jahoda, Horne, & Oliver, 1984; Colin A.B. Jahoda, Reynolds, & Oliver, 1993; Reynolds & Jahoda, 1992). Just above the dermal papilla, the matrix generates stem cells to the growing hair shaft and the root sheath (Plowman et al., 2018). The two regions work together to regulate and carry out hair growth – the dermal papilla is the master controller that instructs the hair-growing engine of the matrix region.

During hair growth, a hair follicle goes through three stages of growth called anagen, catagen, and telogen phases. During the anagen phase, the hair shaft is generated and grows out through the skin, while catagen phase ends hair growth and telogen phase causes the follicle to become dormant (Alonso & Fuchs, 2006).

Changes to several hair-related genes are known to result in hairlessness in specific species. The *Hr* gene in mice, so named because of its role in the hair phenotype, results in hairless mice when knocked-out (Benavides, Oberyszyn, VanBuskirk, Reeve, & Kusewitt, 2009). In Mexican dogs, the *FOXI3* gene has been found to be associated not only with hairlessness, but also associated dental abnormalities (Drögemüller et al., 2008). In the American Hairless Terrier, mutation in a different gene, *SGK3*, is responsible for relative hairlessness (Parker, Harris, Dreger, Davis, & Ostrander, 2017). Fibroblast growth factor genes such as *FGF5* and *FGF7* are also heavily implicated in hair growth because their absence causes drastic changes to coat length and appearance in mice (Ahmad et al., 1998). Such genes are associated with keratinocyte growth in which keratins and keratin-associated proteins play a key role. Unsurprisingly, specific structural proteins that comprise hair shafts and their associated genes, known as *KRTAP* genes or hair-specific keratins, are also heavily implicated in hair-related functions (Plowman et al., 2018). They also appear to be unique to mammals, although some *KRTAP*-like genes have been found in reptiles (Eckhart et al., 2008),

Although genetic changes associated with induced hairlessness in specific domesticated species are useful, it is unclear if such changes reflect evolutionary changes that result in spontaneous hairlessness and how much such changes are convergent across all or many naturally hairless species. By taking advantage of natural biological replicates of independent evolution of hairlessness in mammals, we can learn about global genetic mechanisms underlying the hairless phenotype.

Mammalian hairlessness is a convergent trait since it independently evolved multiple times across the mammalian phylogeny. We can therefore characterize the nature of its convergence at the molecular level to provide insights into the mechanisms underlying the trait. For example, if a gene is evolving quickly in hairless species and slowly in non-hairless species, that implies that the gene may be associated with hairlessness. We focus on the relative evolutionary rate of genomic sequence, which is a measure of how fast the sequence is evolving relative to its expected rate. Unlike seeking sequence convergence to a specific amino acid or nucleotide, using an evolutionary-rates-based method detects convergent shifts in evolutionary rates across an entire region of interest (such as a gene or putative regulatory element).

Evolutionary rate shifts reflect the amount of evolutionary pressure acting on genomic elements, and multiple studies investigating diverse phenotypes have found that phenotypic convergence is indeed associated with convergent changes in evolutionary rates (Chikina, Robinson, & Clark, 2016; Hiller et al., 2012; Hu, Sackton, Edwards, & Liu, 2019; Kapheim et al., 2015; Kowalczyk, Partha, Clark, & Chikina, 2020; Partha et al., 2017; Partha, Kowalczyk, Clark, & Chikina, 2019; Prudent, Parra, Schwede, Roscito, & Hiller, 2016; Wertheim, Murrell, Smith, Kosakovsky Pond, & Scheffler, 2015). We used RERconverge, an established computational pipeline, to link convergently evolving genes and noncoding regions to convergent evolution of mammalian hairlessness. Previous work using RERconverge (Kowalczyk et al., 2019) to detect convergent evolutionary rate shifts in genes and noncoding elements associated with convergently evolving traits has identified the putative genetic basis of the marine phenotype in mammals (Chikina et al., 2016), the fossorial phenotype in subterranean mammals (Partha et al., 2017, 2019), and extreme longevity in mammals (Kowalczyk et al., 2020). Those studies revealed trends that are not species-specific, but instead represent relevant genetic changes that occurred phylogeny-wide.

Here, we further explored the genetic basis of hairlessness across the mammalian phylogeny by finding genes and noncoding regions under relaxation of evolutionary constraint (i.e. evolving faster) in hairless species. Such genetic elements likely have reduced selective constraint in species with less hair and thus accumulate substitutions at a more rapid rate. To find genetic elements under accelerated evolution in hairless species, we performed an unbiased, genome-wide scan across 62 mammal species using RERconverge on 19,149 orthologous genes and 343,598 conserved noncoding elements. In addition to recapturing known hair-related elements, we also identified novel putative hair-related genetic elements previously overlooked by targeted studies. Importantly, newly uncovered genes and noncoding regions were not only related to keratins, but they also represented a suite of genetic functionality underlying hair growth. Such findings represent strong candidates for future experimental testing related to the hair phenotype.

Results

Phenotype Assignment

The hairless phenotype in mammals arose at least nine independent times along the mammalian phylogeny (Figure 1A, Supp. File 1). Genomic regions that experienced evolutionary rate shifts in tandem with mammalian loss of hair were considered potentially associated with phenotype loss. Ten extant and one ancestral hairless species were identified based on species hair density (Figure 1A). Broadly, species with skin visible through hair were classified as hairless, namely rhinoceros, elephant, naked mole-rat, human, pig, armadillo, walrus, manatee, dolphin, and orca. The cetacean (dolphin-orca) ancestor was also included because it was likely a hairless marine mammal.

An ancestral point of phenotypic ambiguity existed at the ancestor of manatee and elephant. Considerable uncertainty exists as to whether the ancestral species had hair and independent trait losses occurred on the manatee and elephant lineages or, alternatively, whether the ancestral species lost hair prior to manatee-elephant divergence and regained hair along mammoth lineages post-divergence (Roca et al., 2009). Since foreground assignment of the manatee-elephant ancestor had little impact on skin-specific signal, we retained the parsimonious assignment of the ancestral species as haired with inferred independent losses in the manatee and post-mammoth elephant lineages (Figure 2B). Similarly, assigning foreground branches based

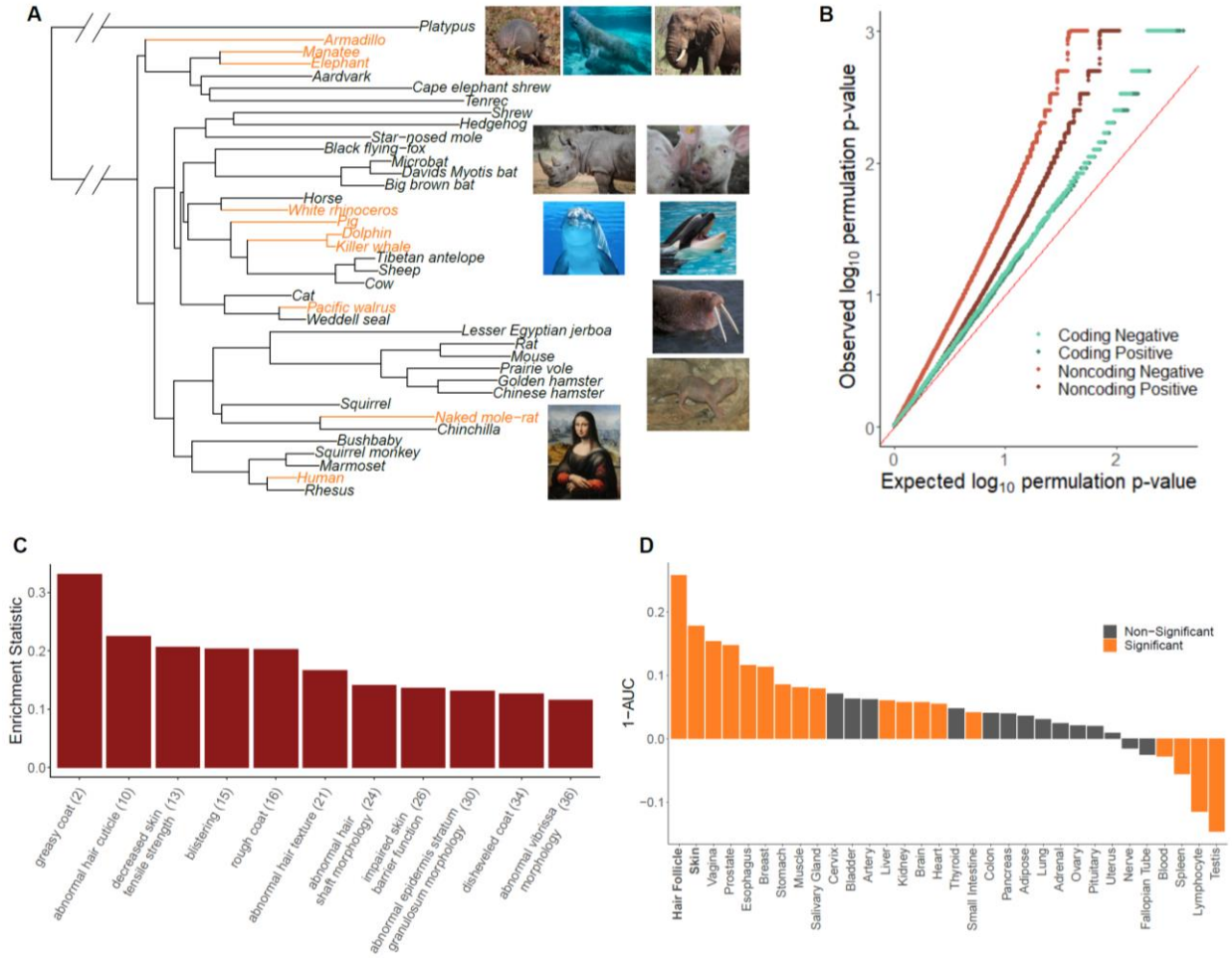

Figure 1. Hairless species show an enrichment of hair-related genes and noncoding elements whose evolutionary rates are significantly associated with phenotype evolution. A) Phylogenetic tree showing a subset of the 62 mammal species used for analyses. Foreground branches representing the hairless phenotype are depicted in orange alongside photographs of the species. B) Q-Q plots for uniformity of permulation p-values for association tests per genetic element for coding and noncoding elements. Shown are both positive associations that indicate accelerated evolution in hairless species and negative associations that indicate decelerated evolution in hairless species. The deviation from the red line (the identity) indicates an enrichment of low permulation p-values – there are more significant permulation p-values than we would observe under the uniform null expectation. This indicates significant evolutionary rate shifts for many genes and noncoding elements in hairless mammals. C) Hair-related MGI category genes are under significantly accelerated evolution in hairless species. Shown are one minus the AUC values (maximum enrichment statistic = 0.5; statistic = 0 indicates no enrichment) for each hair- or skin-related pathway with a permulation p-value less than or equal to 0.01. In parentheses are the statistic-based ranks of those pathways among all pathways under accelerated evolution in hairless mammals with permulation p-values less than or equal to 0.01. D) Skin- and hair-expressed genes are under significant evolutionary rate acceleration in hairless species. All genesets except hair follicle are from the GTEx tissue expression database. Hair follicle genes are the top 70 most highly expressed genes from (Zhang et al., 2017) hair follicle RNA sequencing that are not ubiquitously expressed across GTEx tissue types.

on the state of being hairless or the transition from haired to hairless – i.e. assigning the entire cetacean clade as foreground versus only assigning the cetacean ancestor as foreground – had little impact on skin-specific signal (Figure 2A). In the case of cetaceans, we retained all three branches (orca, dolphin, and the orca-dolphin ancestor) as foreground to maximize statistical power.

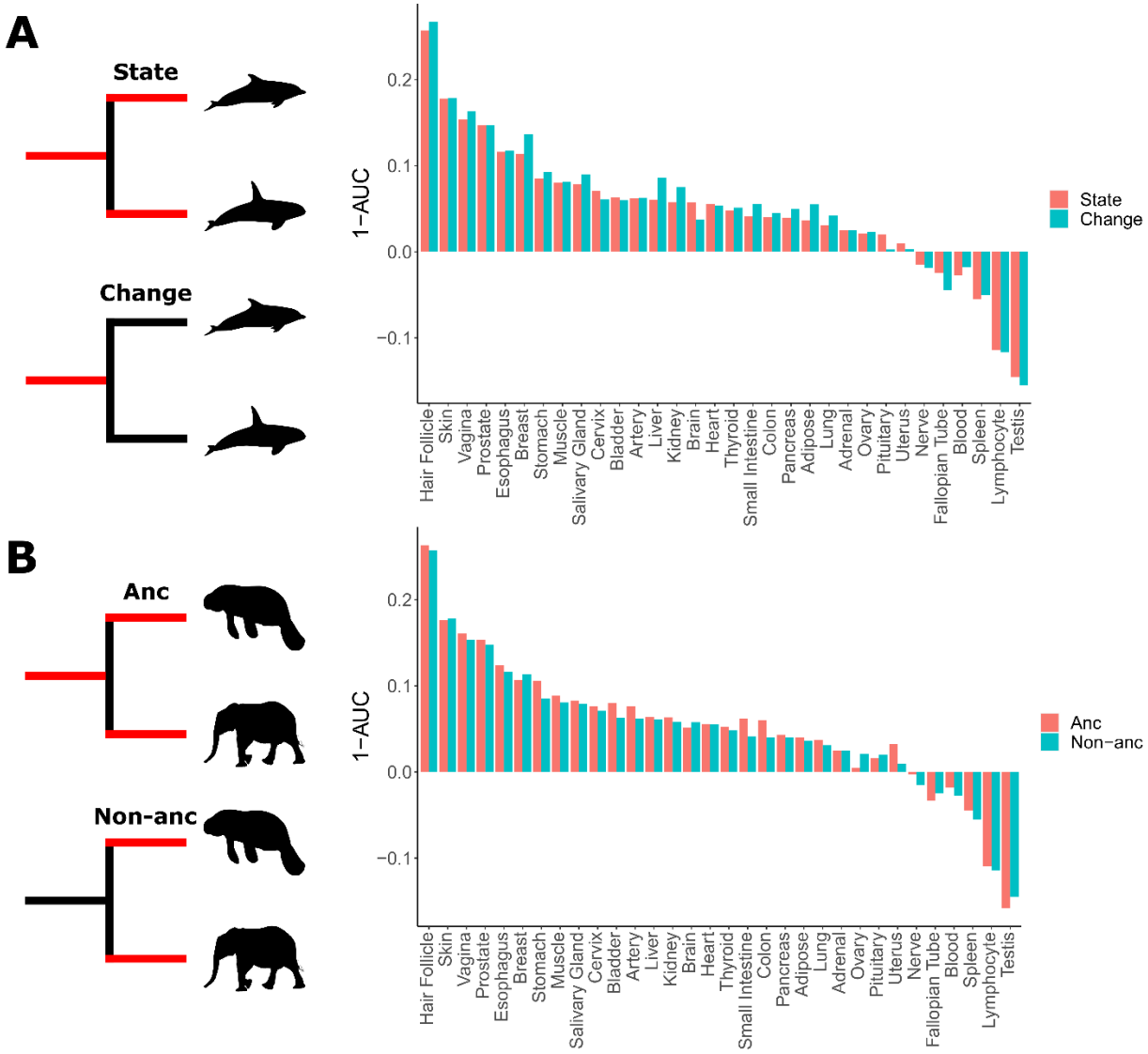

Figure 2. Skin-related genes evolve faster in hairless species. A) When considering either the state of being hairless as the foreground or the process of changing from haired to hairless as the foreground, enrichment of skin-related genes shows little difference. B) When considering the elephant/manatee ancestor as haired or hairless, enrichment of skin-related genes shows little difference.

Phenotypic Confounders

Hairless species share other convergent characteristics that could confound associations between the hairless phenotype and evolutionary rate shifts. In particular, several hairless species are large and many are marine mammals. Therefore, any signal related to hairless species could be driven instead by confounders. Problems with these two confounders were handled in two different ways.

To handle large body size as a confounder, body size was regressed from relative evolutionary rates on an element-by-element basis. In other words, the residuals from the linear relationship between body size and relative evolutionary rates were retained to eliminate the

effect of body size on relative evolutionary rate trend. In doing so, any effects related to the relationship between body size and hairlessness were mitigated.

Marine status, on the other hand, is a trait of potential interest because marine mammals experienced unique hair and skin changes during the transition from a terrestrial to a marine environment. However, it is also of interest how much signal is driven by the marine phenotype versus the hairless phenotype. Therefore, Bayes factors were used to quantify the amount of support for the marine phenotype versus the hairless phenotype. A larger Bayes factor indicated more contribution from one model versus another. A ratio of five or greater for the hairless phenotype versus the marine phenotype indicated strongly more support for signal driven by hairlessness. Many hair-related pathways evolving faster in hairless species according to RERconverge also indicated that signal was indeed driven by the hairless phenotype as opposed to its heavy confounder, the marine phenotype, according to Bayes factor analyses (Figure 3).

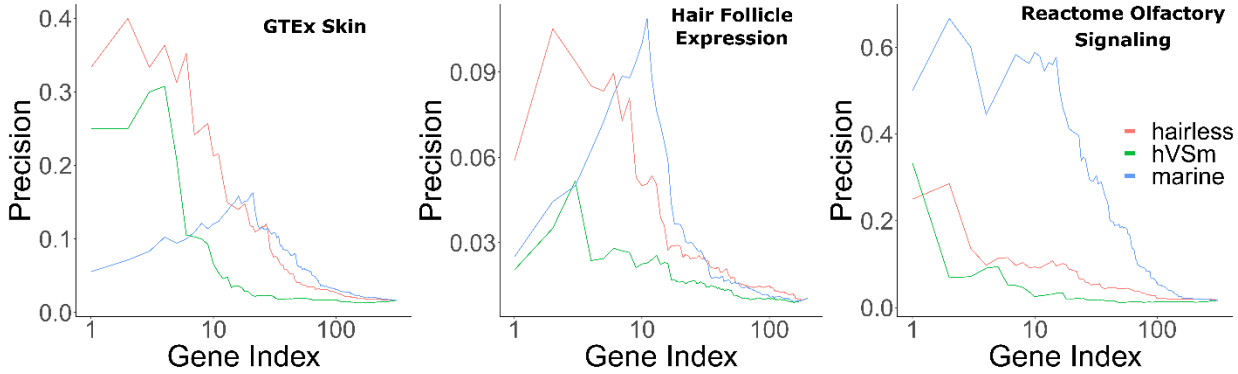

Figure 3. Bayes factors reveal the proportion of signal driven by the marine phenotype versus the hairless phenotype. Depicted are precision-recall curves demonstrating how Bayes factors of the contrasting hairless and marine phenotypes rank genes related to skin, hair, and olfaction. Also plotted is a ranking based on the ratio of hairlessness and marine Bayes factors (hVSm = hairlessness Bayes factor/marine Bayes factor). The ratio of the Bayes factors quantifies the amount of support for the hairless phenotype beyond the support for the marine phenotype per gene. In other words, a high Bayes factor ratio indicates a signal of evolutionary convergence associated with hairlessness that is not only driven by signals of convergence in hairless marine mammals. The hairless phenotype had much greater power to enrich for genes expressed in skin (GTEx data) compared to the marine phenotype, indicating that accelerated evolution is driven more strongly by hairlessness. Both the marine and hairless phenotypes enriched for genes in hair follicle expression genes, indicating that both contribute to accelerated evolution of those genes. Olfactory genes on the other hand are expected to show acceleration only related to the marine phenotype. As expected, the marine phenotype much more strongly enriched for olfactory genes than the hairless phenotype.

Known Hair-Related Genetic Elements Evolve Faster in Hairless Species

We used RERconverge to identify genes and noncoding elements evolving at significantly faster or slower rates in hairless species compared to haired species (see Methods). Briefly, the evolutionary rates of genetic elements were compared in hairless versus haired species using a rank-based hypothesis test, and we generated p-values empirically with a newly developed method, termed permulations, that uses phylogenetically constrained phenotype permutations (Saputra, Kowalczyk, Cusick, Clark, & Chikina, 2020). The permulation method compares the correlation statistics from the true phenotype to correlation statistics that arise from randomized phenotypes that preserve the relative species relationships. Thus, small p-values indicate a specific association with the hairless phenotype.

We find that quantile-quantile (QQ) plots of permulation p-values from hypothesis tests for all genetic elements indicate a large deviation from the expected uniform distribution and thus an enrichment of significant permulation p-values (Figure 1B, Supp. File 2 and 3). We show enrichment of significant p-values for both positive and negative evolutionary rate shifts, and the direction of the rate shifts is critical to interpretation. Positive rate shifts imply rate acceleration, which we interpret as a relaxation of evolutionary constraint. While positive rate shifts could theoretically be driven by positive selection, we demonstrate that this is not the case for our top accelerated genes. Branch-site models to test for positive selection were performed using PAML (Yang, 2007) on top accelerated genes. Tests showed little evidence for foreground-specific positive selection; out of 199 genes tested, 27 genes demonstrated hairless acceleration, but all such genes also showed evidence for tree-wide positive selection, suggesting that positive selection was not specific to hairless species although perhaps stronger (Supp. File 4). Thus, regions with positive rate shifts evolve faster in hairless species due to relaxation of evolutionary constraint, perhaps because of reduced functionality driving or in conjunction with the hairlessness phenotype. Negative rate shifts indicate increased evolutionary constraint in hairless species, which implies increased functional importance of a genomic region. While negative shifts are more difficult to interpret in the context of trait loss, they may represent compensatory phenotypic evolution in response to trait loss.

To demonstrate that the statistical signal from individual genes and noncoding regions is meaningful, we evaluated to what extent those RERconverge results enrich for known hair-related elements. We calculated pathway enrichment statistics using a rank-based test and statistics from element-specific results to evaluate if genes or noncoding elements that are part of a predefined biologically coherent set are enriched in our ranked list of accelerated regions. Using numerous gene sets associated with hair growth, such as KRTs, KRTAPs, hair follicle expressed genes (Zhang et al., 2017), skin-expressed genes (Papatheodorou et al., 2018), and Gene Ontology (GO) (Ashburner et al., 2000), Mouse Genome Informatics (MGI) (Eppig et al., 2015), and canonical hair-annotated genes (Liberzon et al., 2011), we indeed find that our results are highly enriched for hair-related functions (Supp. File 5). As shown in Figure 1C, many of the top-enriched MGI phenotypes are hair-related. Likewise, enrichment analyses using the GTEx tissue expression database (Papatheodorou et al., 2018) supplemented with hair follicle expressed genes (Zhang et al., 2017) show strong enrichment for both skin and hair follicle genes, as well as signal for other epithelial tissues such as vagina and esophagus (Figure 1D).

Hair-related pathways remained enriched among rapidly evolving genes even when KRTs and KRTAPs were removed (Supp. File 6). This implies that hairless-related genetic changes are not merely structural, but instead they are broadly driven by many genes related to the hair cycle. Similarly, no individual hairless species had an undue impact on enrichment of known hair-related pathways as indicated by consistent findings when individual hairless species were removed from analyses (Figure 4).

Investigating a focused list of gene sets associated with specific structures of the hair follicle revealed an interesting contrast between coding and noncoding sequence (Figure 5). Significantly accelerated genes were primarily within the hair shaft itself for coding sequence. Noncoding regions near genes related to the hair shaft were also under accelerated evolution, and additionally, noncoding regions near genes for the matrix and dermal papilla also showed patterns of decelerated and accelerated evolution, respectively, in hairless species. Since the matrix and dermal papilla play key roles in hair follicle localization, development, and cycling, evolutionary rate shifts in those compartments' noncoding regions suggests that regulatory

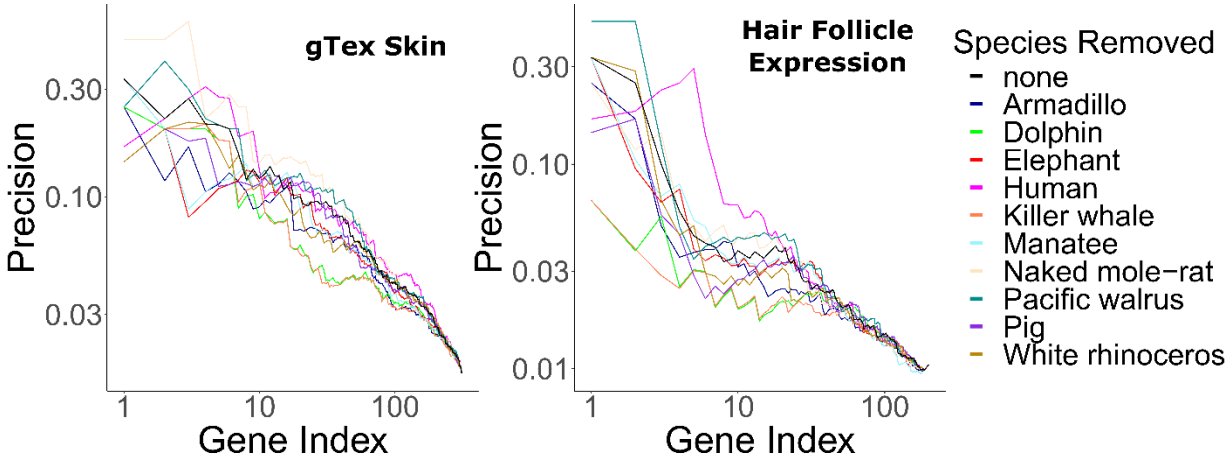

Figure 4. Hair-related pathways are enriched for genes with evolutionary rates significantly accelerated in hairless species. Enrichment is consistent even when individual hairless species are removed.

sequence evolution rather than coding sequence evolution may drive changes in hair follicle formation.

Overall, these results indicate strong enrichment for hair-related function in both protein coding genes and non-coding regions that are convergently accelerated in hairless species.

Analyses Reveal Novel Putative Hair-Related Genetic Elements

After extensive filtering using RERconverge statistics, Bayes Factors, and permulation statistics, several novel putatively hair-related genes were uncovered. Shown in Table 1, the top accelerated gene associated with hairlessness with strong support for hairless-related signal as opposed to marine-related signal was *FGF11*. While *FGF11* has no known role in hair growth, its expression is highly enriched in the skin and other fibroblast growth factor genes are known to be related to hair growth (Kawano et al., 2005; Lee et al., 2019; Nakatake, Hoshikawa, Asaki, Kassai, & Itoh, 2001; Rosenquist & Martin, 1996; Suzuki, Ota, Ozawa, & Imamura, 2000). Together these observations support *FGF11* as another strong candidate for hair-related function.

The second-ranked gene, *GLRA4*, a glycine receptor subunit, is more difficult to interpret because while generally conserved across mammals, it is a pseudogene in humans, so it has been relatively less studied. Glycine receptors are often involved in motor reflex circuits (Callister, 2010), and thus with respect to any functional relevance to hair we hypothesize that GLRA4 may contribute to regulating the reflexive piloerection response (hairs "standing on end") observed in many mammals.

Other top-accelerated genes are *KRT2*, *KRT35*, *PKP1*, and *PTPRM*, all of which are known hair-related genes. *KRT2* protein product localizes in the hair follicle and may play a role in hair and skin coloration (Cui et al., 2016), and *KRT35* is a known target of *HOXC13* and is essential for hair differentiation (Lin et al., 2012). *PKP1* mutations lead to ectodermal dysplasia/skin fragility syndrome, which includes abnormalities of both skin and hair development (Sprecher et al., 2004). *PTPRM* regulates cell-cell communication in keratinocytes (Peng et al., 2015).

The remaining accelerated genes are also plausibly connected to skin- and hair-related functions. *ANXA11* has been strongly linked to sarcoidosis in humans (Hofmann et al., 2008), an inflammatory disease in epithelial tissue. *MYH4*, a myosin heavy-chain protein, has surprisingly also been implicated in skin and hair growth, both through upregulation during hair follicle

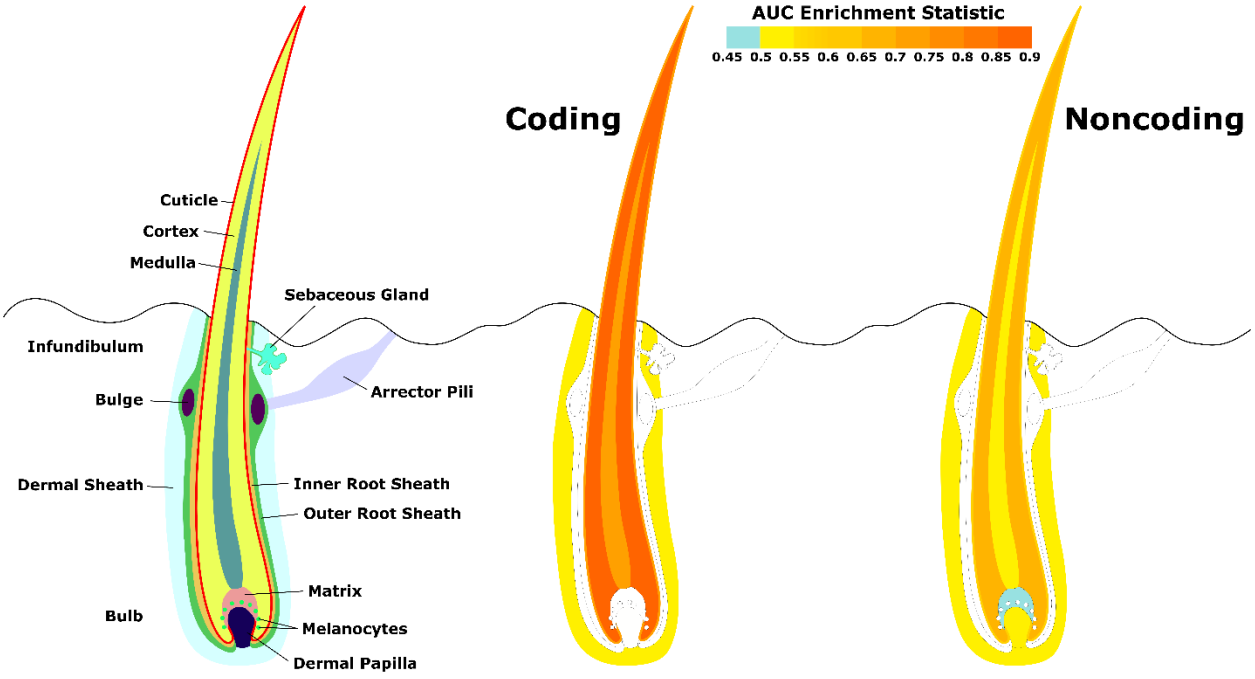

	Coding				Noncoding			
	p-value	adjusted p-value	AUC	Number of Genes	p-value	adjusted p-value	AUC	Number of CNEs
Cortex	0.00042	0.0050	0.86	8	4.20e-7	2.94e-6	0.65	93
Cuticle	0.010	0.035	0.72	11	1.58e-7	2.21e-6	0.59	287
Medulla	0.0059	0.028	0.72	13	5.80e-3	2.71e-2	0.55	263
Inner Root Sheath	0.15	0.41	0.60	19	0.54	0.66	0.51	626
Bulge	0.34	0.52	0.57	15	0.25	0.50	0.48	397
Outer Root Sheath	0.30	0.52	0.56	28	0.55	0.66	0.49	695
Matrix	0.71	0.90	0.55	4	0.078	0.18	0.46	191
Dermal Sheath	0.00072	0.0050	0.55	436	0.059	0.16	0.50	13482
Arrector Pili	0.30	0.52	0.54	45	0.39	0.66	0.51	2421
Sebaceous Gland	0.21	0.48	0.54	94	0.75	0.75	0.50	2709
Bulb	0.96	0.96	0.50	12	0.57	0.66	0.49	470
Infundibulum	0.87	0.94	0.48	7	0.73	0.75	0.51	218
Dermal Papilla	0.88	0.94	0.48	5	0.049	0.16	0.55	139
Melanocytes	0.52	0.72	0.46	19	0.48	0.66	0.49	663

Figure 5. Diagram of hair shaft and follicle with shading representing region-specific enrichment for coding and noncoding sequence. Both coding and noncoding sequence demonstrate accelerated evolution of elements related to hair shaft (cortex, cuticle, and medulla). Noncoding regions demonstrate accelerated evolution of matrix and dermal papilla elements not observed in coding sequence. All compartment genesets were compiled from MGI annotations that contained the name of the compartment except arrector pili (Santos et al., 2015) and dermal sheath (Heitman et al., 2020) genesets.

Gene	Statistic	p-adj	BF HvM	BF Hairless	BF Marine	Perm p-adj	Noncoding Enrich Stat	Noncoding Enrich p-adj
FGF11	0.403	0.205	116.4	6354.7	54.6	0.201	-0.115	0.051
GLRA4	0.332	0.179	22.6	1908.3	84.3	0.201	-0.159	0.068
ANXA11	0.328	0.179	25.5	45.2	1.8	0.201		
PTPRM	0.326	0.179	51.7	4393.6	85.0	0.201	0.146	1.19e-9
PKP1	0.323	0.179	5.6	2669.0	478.9	0.201	0.117	0.410
KRT2	0.304	0.205	2235.7	27034.4	12.1	0.201	0.175	0.181
MYH4	0.297	0.205	28.0	11447.2	409.3	0.201	0.147	0.311
KRT35	0.293	0.205	8.6	1954.5	227.3	0.201	0.142	0.211

Table 1. Genes whose evolutionary rates are significantly associated with the hairless phenotype with significant parametric p-values, significant permulation p-values, positive statistic, and hairless versus marine Bayes factors (BF) greater than five. BF Marine and BF Hairless are bayes factors for those phenotypes individually, while BF HvM is the ratio of the two (BF Hairless/BF Marine). The ratio of the Bayes factors quantifies the amount of support for the hairless phenotype beyond the support for the marine phenotype per gene. In other words, a high Bayes factor ratio indicates a signal of evolutionary convergence associated with hairlessness that is not only driven by signals of convergence in hairless marine mammals. Also shown are enrichment statistics for noncoding regions near top genes. Adjusted p-values are Benjamini-Hochberg corrected. Note that permulation p-values observed as 0 were adjusted to 0.001 (the smallest observable permulation p-value) prior to multiple hypothesis testing correction. Cells with missing values (for "Noncoding Enrich Stat" and "Noncoding Enrich p-adj") do not have enough observations to calculate enrichment statistics because too few conserved noncoding elements were detected in the vicinity of those genes.

cycling and skin healing (Carrasco et al., 2015) and upregulation in response to overexpression glucocorticoid receptors that drive hair follicle morphogenesis (Donet, Bayo, Calvo, Labrie, & Pérez, 2008). Note that in both cases of *MYH4* upregulation, it was the only myosin with significantly different expression in the tissues studied, suggesting a unique role for the protein in skin and hair growth.

In addition to identifying genes with significant evolutionary rate shifts in coding sequence, we have also found many other protein-coding genes with significant enrichment of hairless-accelerated non-coding elements in their vicinity (https://pitt.box.com/s/b8ozkcwzile4znq8tw9ri8s160zjb3uw and Figure 6). There is a global trend in correlation between evolutionary rate shift statistics for protein-coding regions and enrichment statistics for their nearby non-coding regions (Pearson's Rho = 0.177). Concordance between accelerated evolutionary rates in genes and their nearby noncoding regions is particularly strong for *KRT*s and *KRTAP*s, which are known to be skin- and hair-related (Figure 6B) – out of 69 *KRT*s and *KRTAP*s for which noncoding enrichment could be calculated, 66 showed accelerated evolution in both protein-coding sequence and non-coding regions. However, across all genes with strong signals for nearby noncoding regions under accelerated evolution in hairless mammals (permulation p-value less than or equal to 0.03), acceleration in the coding sequence itself spans a wide range of values (Figure 6A), and in many cases there is little evidence of evolutionary rate shifts in the coding sequence. This range likely reflects the requirement that some protein-coding sequences remain under strong evolutionary constraint because of their continued importance in non-hair-related tissues.

Top-ranked genes with accelerated nearby noncoding regions include several known hair-related regulator genes (*ELF3*, *FOXC1*, and others) (Figure 6C). *FOXC1* is a transcription factor involved in maintaining the hair follicle stem cell niche (Lay, Kume, & Fuchs, 2016; L. Wang,

Siegenthaler, Dowell, & Yi, 2016) and *ELF3* is known to regulate transcription of keratin genes (Aldinger et al., 2009). These genes showed no coding region acceleration, which is expected since they are highly pleiotropic. Regulatory proteins tend to have many functions – for

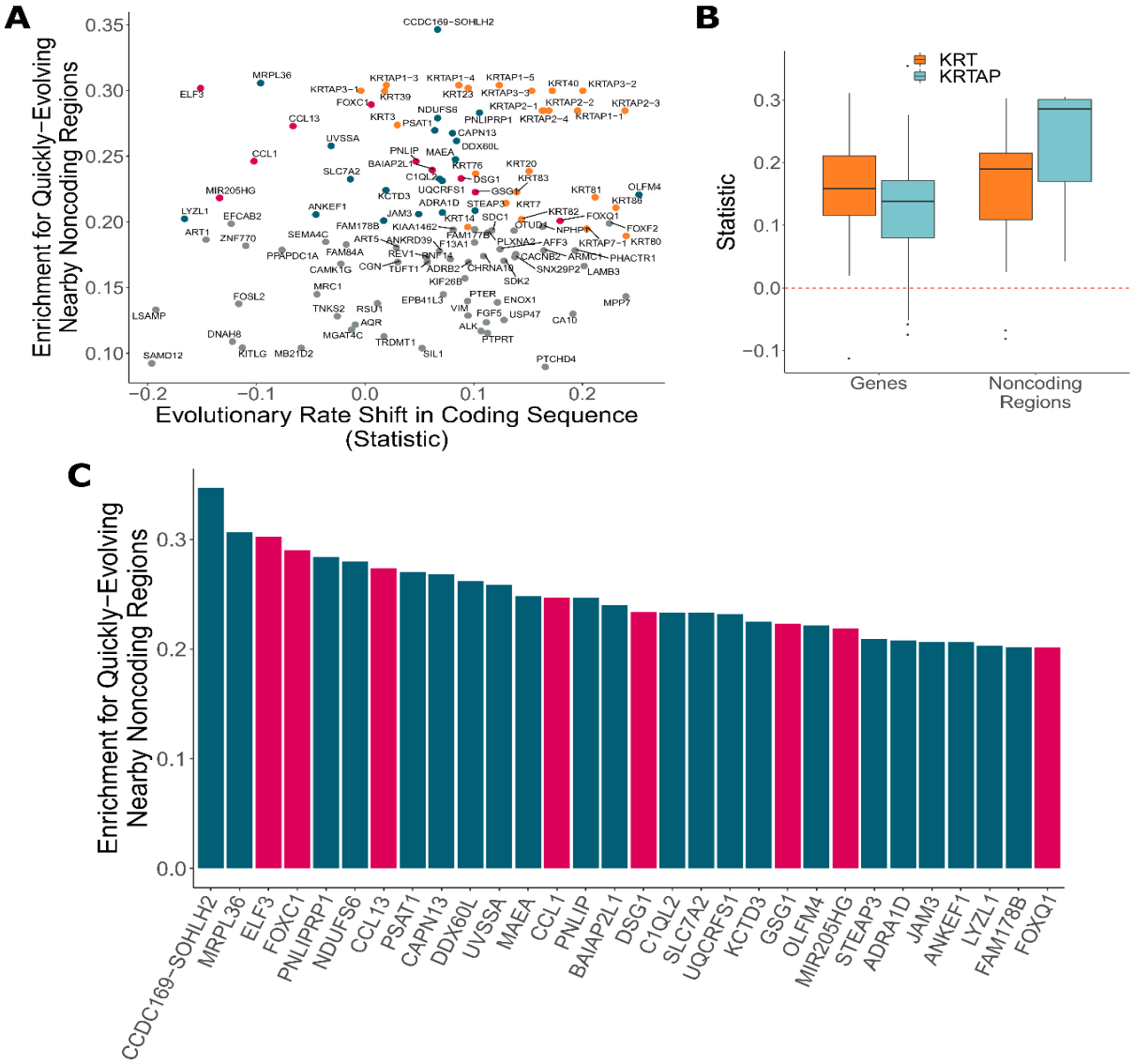

Figure 6. Noncoding regions near hair-related genes evolve faster in hairless species. A) Genes with a significant enrichment for quickly evolving nearby noncoding regions (permulation p-value of 0.03 or less) only sometimes demonstrate evolutionary rate shifts in their protein-coding sequences. In orange are keratins and keratin-associated proteins, which tend to show accelerated evolutionary rates in both genes and nearby non-coding regions. In pink are top genes also in pink in panel C. In blue are all other genes in panel C. B) Keratin (*KRT*) and keratin-associated protein (*KRTAP*) genes and nearby noncoding sequence show enrichment for accelerated evolutionary rates. Show are rate shift statistics for genes and enrichment statistics for noncoding regions. C) Many top-ranked genes for nearby quickly evolving noncoding regions are hair-related. Depicted are the top 30 genes (*KRT*s and *KRTAP*s excluded) based on enrichment statistic with enrichment permulation p-value of 0.03 or less. No genes had significant evolutionary rate shifts in coding sequence except *OLFM4*, which evolves faster in hairless species. In pink are genes with hair-related functions in the literature (citations: *ELF3* (Blumenberg, 2013), *FOXC1* (Lay et al., 2016), *CCL13* (Michel et al., 2017; Suárez-Fariñas et al., 2015), *CCL1* (Nagao et al., 2012), *DSG1* (Zhang et al., 2017), *GSG1* (Aya, Shimokawa, & Doi, 2009), *MIR205HG* (D. Wang et al., 2013), *FOXQ1* (Ashburner et al., 2000; Carbon et al., 2019)).

A

	Statistic	p-adj
MIR205	0.238	8.6e-10
MIR1305	0.162	1.1e-6
MIR924	0.178	6.8e-6
MIR124-1	0.218	2.4e-5
MIR346	0.283	2.4e-5
MIR759	0.152	8.3e-5
MIR3167	0.150	2.1e-4
MIR4255	0.189	4.4e-4

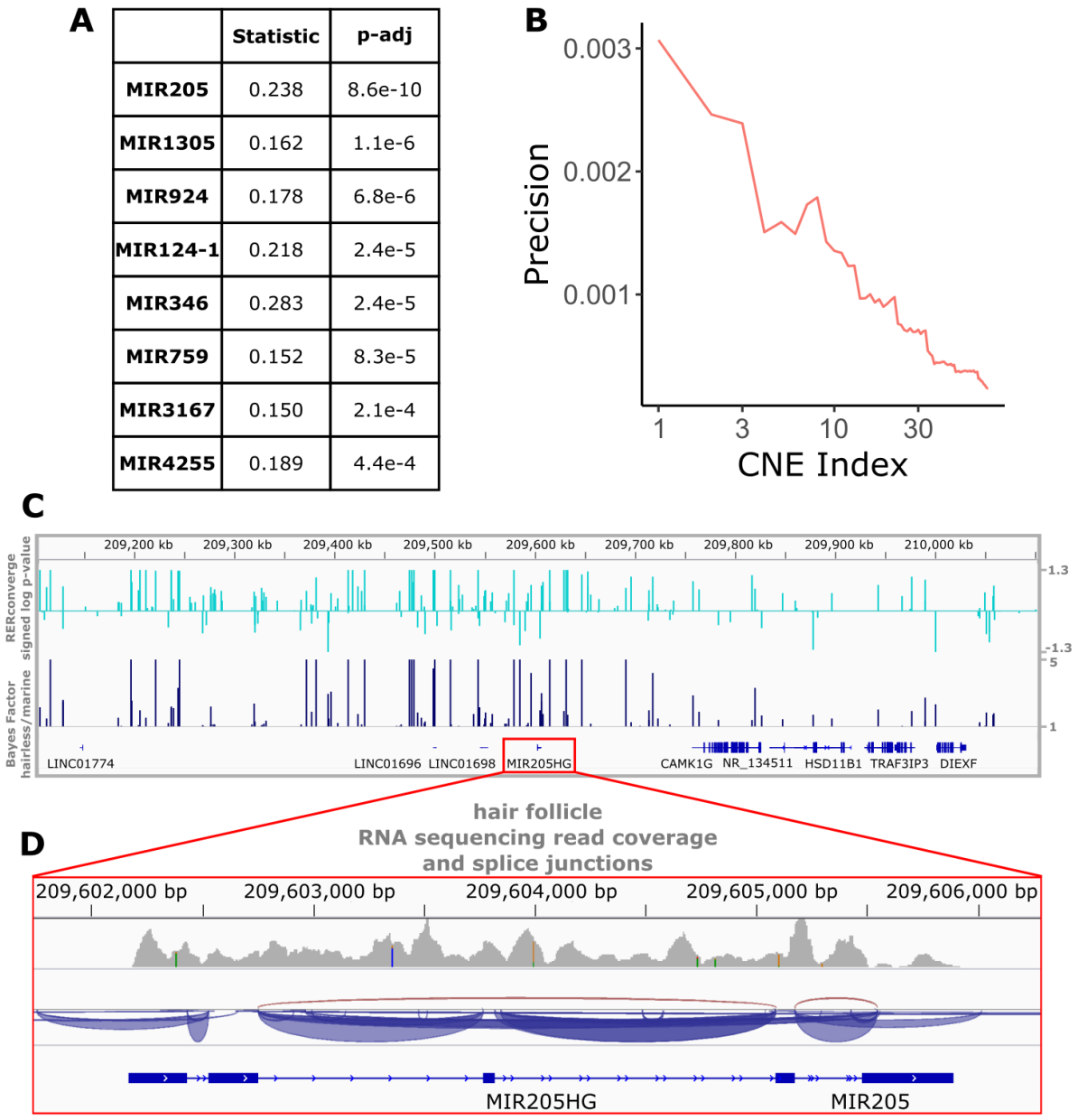

Figure 7. Top miRNAs with nearby noncoding regions with evolutionary rates significantly associated with the hairless phenotype. A) Wilcoxon rank-sum enrichment statistics and Benjamini-Hochberg corrected p-values for top-ranked miRNAs. B) Precision recall curve of statistic ranks for CNEs near *mir205* demonstrates an enrichment of CNEs with accelerated evolution near *mir205* compared to all noncoding regions near microRNAs. C) The chromosomal region around *mir205* shows a large number of CNEs accelerated in hairless species, as seen for RERconverge and Bayes factor scores. Note the relative decline of peaks in the vicinity of nearby protein-coding genes such as *CAMK1G* to the right. D) *mir205* is well-known to be associated with hair and skin growth and structure. Its transcriptional unit on chromosome 1 shows clear read pileups from hair follicle RNAseq data (Zhang et al., 2017). Gray peaks represent the number of RNAseq read coverage and blue curves represent splice junctions.

example, in addition to their hair-related functions, *FOXC1* regulates embryonic development (Brembeck, Opitz, Libermann, & Rustgi, 2000; Seo et al., 2006) and *ELF3* is involved in the epithelial to mesenchymal transition (Sengez et al., 2019) – so we expected to observe no loss of constraint in the coding sequence for those proteins. Instead, changes to regions that regulate

expression of those regulatory proteins appear to be driving the convergent evolution of hairlessness. While regulation of transcription factor expression is highly complex, our analysis pinpoints regions that are candidates for hair-specific regulation.

The global analysis of noncoding regions also revealed under-characterized regions (*CCDC162-SOHLH2*, *FAM178B*), and regions that may plausibly be connected to hair or skin (*UVSSA* (Sarasin, 2012), *OLFM4* (Jaks et al., 2008; Muñoz et al., 2012), *ADRA1D* (Rezza et al., 2016)). These noncoding regions are excellent candidates for further experimental analyses to explore their role in regulating hair and skin growth, development, and cycling.

Perhaps even more so than genes and their regulatory regions, microRNAs are strong candidates for hair-related functions. A key component of hair follicle cycling is persistence of stem cells, and microRNAs are known to be important players in stem cell regulation (Peng et al., 2015). Too small to be analyzed via their sequence alone using our analysis strategy, we mapped noncoding regions to nearby microRNAs and performed enrichment analyses to identify groups of microRNA-associated noncoding regions enriched for significant association with the hairlessness phenotype (Figure 7A). The top enriched microRNA with rapidly evolving nearby noncoding regions was mir205, a microRNA known to be associated with skin and hair development (D. Wang et al., 2013). *Mir205* is readily studied because its host gene (*mir205hg*) is long enough to be captured using standard methods, including bulk RNA sequencing. Reanalyzed data from a previous study (Zhang et al., 2017) focused on coding sequence revealed read pileups at *mir205hg* even without microRNA-specific capture methods (Figure 7C and D). Through our study, we now know which noncoding regions in the gene desert around *mir205* potentially control its expression in hair follicles as opposed to other tissues. Through this scan for associated noncoding elements, we similarly identified several poorly characterized microRNAs with significant hair-related signal that are less studied and are also strong candidates for hair-related functions (Figure 7A). Furthermore, we have identified the precise noncoding regions that likely control their expression in the context of hair and hair follicles (Supp. File 5).

Discussion

These analyses successfully used RERconverge, a method to link convergent evolutionary rates of genetic elements with convergent phenotypes, to identify known hair-related genes in mammals. In addition to identifying known genes, other understudied genes and microRNAs were also identified as key plausible targets for further inquiry into the genetic basis of hairlessness, and a suite of putative regulatory elements associated with hair and skin were uncovered.

The top-ranked gene was *FGF11*, a fibroblast growth factor gene. It evolved faster in hairless species due to relaxation of evolutionary constraint, indicating that it has reduced functionality in hairless species. Fibroblast growth factors are readily studied for a variety of functions, but the precise functionality of *FGF11* is unknown. The gene may be associated with cancer development through interaction with T-cells (Ye et al., 2016), and it has also been implicated in tooth development in mice (Kettunen, Furmanek, Chaulagain, Hals Kvinnsland, & Luukko, 2011). Interestingly, the gene related to hairlessness in Mexican Hairless dogs is also related to dentition (Drögemüller et al., 2008), implying plausibility for a hair-related gene to also be tooth-related. Furthermore, numerous fibroblast growth factor genes have been studied in relation to hair growth (Rosenquist & Martin, 1996), including work that found errors in *FGF5* resulted in longer hair in goats (Li et al., 2019), *FGF5* and *FGF7* regulation controlled

hair anagen phase in mice (Lee et al., 2019), and *FGF2* stimulated hair growth when applied to mouse skin (Xu, Chen, Wang, Xue, & Fu, 2018). *FGF11* is an excellent candidate to perform similar tests for hair-related functions, among other high-scoring genes in the list such as *MYH4* and *ANXA11*.

Compared to coding sequence, study of noncoding regions is more challenging for several reasons. First, identifying such regions genome-wide is difficult because they lack the defining characteristics that genes share, such as start and stop codons, and thus finding putative regulatory elements using sequence alone is an ongoing area of study. Our strategy of using conserved regions as putative regulatory elements likely misses many real regulatory sequences while simultaneously capturing conserved elements with no regulatory function. However, our method is also unbiased and provides a robust set of sequences to analyze, many of which likely do have regulatory functions. Second, validating our findings from noncoding regions is difficult because few CNEs have known functions. Therefore, to validate our noncoding results, we mapped noncoding regions to nearby genes and inferred CNE functions based on the functions of those genes. Such proximity-based mapping has known flaws because enhancers can have distal effects and chromatin state controls enhancers' access to genes regardless of distance. However, despite all of the potential sources of error, we identify global signal for noncoding regions under accelerated evolution in hairless species (Figure 1B) and signal for hair-related acceleration of noncoding regions (Figures 5, 6, and 7).

Further analyses of noncoding regions revealed an interesting deviation from signals of accelerated evolution in coding regions. Namely, coding regions primarily showed acceleration in genes related to texture and the structure of the hair shaft itself. Noncoding regions, on the other hand, showed accelerated evolution near genes related to the dermal papilla and the matrix. Both regions are essential for hair growth. The dermal papilla is the master controller of hair follicle development and hair growth, and it has in fact been repeatedly shown to be sufficient to cause hair growth. Dermal papilla cells, when transplanted to hairless skin such as footpads, has consistently been shown to result in development of hair follicles (C. A.B. Jahoda et al., 1984; Colin A.B. Jahoda et al., 1993; Reynolds & Jahoda, 1992). Since all mammals are capable of growing hair and do have at least some hair at some point in their life cycles, these findings imply that function of genes related to the dermal papilla must be preserved, and spatial and temporal changes in hair growth may be driven by noncoding regions. Much like the dermal papilla, the hair follicle matrix is essential for hair growth – mitotically-active matrix cells give rise to all other inner hair structures, including the hair shaft and the root sheath. Early-stage matrix differentiation can even progress without dermal papilla signaling (Mesler, Veniaminova, Lull, & Wong, 2017). Hair cannot exist without the dermal papilla and matrix, and alterations to their related noncoding regions could plausibly have a large impact on hair growth capabilities. Changes to their associated regulatory regions, on the other hand, may be more flexible and allow for the changes in hair localization, texture, and density that we observe in near-hairless mammals.

Other genes with nearby accelerated noncoding regions likewise demonstrate conservation in protein-coding sequence, possibly because of strong pleiotropy of hair- and skin-related genes. In fact, among the top-ranked non-keratin genes with quickly evolving nearby noncoding regions, only one gene showed a significant evolutionary rate shift in protein-coding sequence (Figure 6). *FOXC1* and *ELF3*, among the top-ranked genes, are strongly linked to hair and skin development (Brembeck et al., 2000; Lay et al., 2016; L. Wang et al., 2016) but also have other essential functions (Aldinger et al., 2009; Sengez et al., 2019; Seo et al., 2006). Our

findings imply that many hair-related genes may have similar pleiotropy preventing accelerated evolution of coding sequence in hairless species. Instead, plasticity of gene regulation through accelerated evolution of noncoding regions may allow for the evolution of hairlessness.

Additionally based on noncoding sequences near regions of interest, mir205 was found to be the top-ranked microRNA with nearby noncoding sequences under accelerated evolution. Mir205 is well-established microRNA related to hair and skin development (D. Wang et al., 2013), and it thereby serves as a strong validation that signals of convergent evolution are successfully identifying hair-related elements. The second-ranked mir1305 has been implicated in skin functionality with significantly different expression levels in damaged versus healthy skin (Liang et al., 2012). Numerous microRNAs have been implicated in hair- and skin-related functions (Andl & Botchkareva, 2015; Fu, Zhao, Zheng, Li, & Zhang, 2014), likely a subset of the total elements involved in hair growth. In general, microRNAs are likely key players in hair follicle cycling because of their importance in stem cell regulation (Peng et al., 2015), and the microRNAs and their associated noncoding regions identified in this work serve as a valuable list of candidates for further inquiry. Likewise, noncoding regions near other hair-related genes are also under accelerated evolution in hairless species and may regulate hair- and skin-related functions. Further, some under-characterized and plausibly hair- and skin-related genes, such as *CCDC169-SOHLH2* and *FAM178B*, have nearby accelerated noncoding regions and thus identify those genes and their regulatory regions as candidates for further experimental testing.

This study has revealed a slew of fresh candidate genes, noncoding regions, and microRNAs putatively associated with hair growth. As an unbiased, genome-wide scan across a large swath of the mammalian phylogeny, it represents not only a step toward fully understanding hair growth, but also understanding the evolution of hair across all mammals.

Acknowledgements

We would like to thank Dr. Andreas Pfenning and Dr. Dennis Kostka for helpful feedback, as well as Elysia Saputra, Weiguang Mao, and all members of the Clark and Chikina labs for helpful feedback.

Funding

Funding for this research was provided through National Institutes of Health grants R01HG009299, R01EY030546, and U54 HG008540.

Methods

Calculating body size-regressed relative evolutionary rates

The RERconverge package in R was used to generate phylogenetic trees for each gene and noncoding region in which branch length represented the amount of evolutionary change, or the number of nonsynonymous substitutions, that occurred along that branch as described in several previous publications (Kowalczyk et al., 2019, 2020; Partha et al., 2019). Alignments for 19,149 genes in 62 mammal species were obtained from the UCSC 100-way alignment (Blanchette et al., 2004; Harris, 2007; Kent et al., 2002). The topology used to generate element-specific trees is included below under "Phylogenetic Trees".

Likewise, alignments for 343,598 conserved noncoding elements were extracted based on phastCons conservations scores across the 62 mammal species and the blind mole-rat (*Nanospalax galili*) (Siepel et al., 2005). Briefly, the full set of conserved elements across 46 placental mammals and their respective phastCons scores were downloaded from the UCSC genome browser (Kent et al., 2002) from the hg19 (human genome) "Cons 46-way" track (phastConsElements46wayPlacental). Regions that overlapped coding regions were removed using the UCSC genome browser "Intersection" utility and the "Genes and Gene Predictions" annotations from the "GENCODE V28lift37" track. Elements with phastCons scores greater than 350 were maintained, and elements less than 10 base-pairs apart were merged. Finally, elements with fewer than 40 base-pairs were discarded to result in the final 343,598 regions. Orthologs for all 63 mammals were downloaded from the UCSC 100-way alignment. Blind mole-rat elements were added based on the pairwise alignment between hg38 (human genome) and *Nannospalax galili* genome (Zerbino, Wilder, Johnson, Juettemann, & Flicek, 2015) by first mapping hg19 coordinates to hg38 coordinates (Supp. File 7 and 8). Orthologs were added to the 62 mammal species alignments using MUSCLE (Edgar, 2004). Data generation steps and code are available here: https://pitt.app.box.com/notes/488875889604.

Alignments were used to generate evolutionary rate trees based on a well-established topology of the mammalian phylogeny in the Phylogenetic Analysis by Maximum Likelihood (PAML) program (Meyer et al., 2018; Yang, 2007). Briefly, RERconverge was used to convert evolutionary rate information from each gene- or noncoding element-specific tree by correcting for the mean-variance relationship among branch lengths and normalizing each branch for the average evolutionary rate along that branch such that the final branch length was relative to the expectation for that branch (Partha et al., 2019).

The resulting relative evolutionary rates were used to calculate body size-regressed relative evolutionary rates. Using adult weight information for the 62 mammal species obtained from the Anage Animal Aging and Longevity Database (Tacutu et al., 2018), RERconverge functions were used to predict body size phenotype values throughout the mammalian phylogeny. Residuals from a linear model fitted to the phenotype values and the relative evolutionary rates for each gene and conserved noncoding element were extracted and used as the body size-regressed relative evolutionary rates for that element.

RER matrices and phylogenetic trees are available at:
https://pitt.box.com/s/newoupek4nlfnx1y5xri7xnx9i96ir9s

Defining hairless species

Since all mammals have some hair during at least one stage of life, no species are truly hairless. Therefore, classification of species as "hairless" versus "haired" was qualitatively

based on density of hair covering and quantitively based on the impact of removing species on the hair-related signal detected during analyses. Tendency was the err on the side of leniency when assigning species as hairless – any species with reduced hair quantity was classified as hairless.

Extant species classified as hairless were armadillo, elephant, white rhinoceros, pig, naked mole-rat, human, and marine mammals (manatee, pacific walrus, dolphin, and orca). The hairless set comprised all but one marine mammal in the 62 mammal species (the furry Weddell seal is not included in the hairless set). The only non-extant species classified as hairless was the orca-dolphin ancestor (the cetacean ancestor) because that species was likely also a hairless marine species (Z. Chen et al., 2013; Nery et al., 2014). The elephant-manatee ancestor was not classified as hairless because modern elephants have known extinct hairy sister species (wooly mammoths) that diverged after the elephant-manatee divergence (Roca et al., 2009). Thus, classifying the elephant-manatee ancestor as hairy was the most parsimonious phenotype assignment for the afrotherian clade. The classification was also supported by the data, which indicated a stronger signal for skin-related genes when the elephant-manatee ancestor was classified as hairy (Figure 2).

Although some species are undeniably hairy (dog, cat, sheep, etc.) and some are undeniably relatively hairless (orca, dolphin, elephant, etc.), some species are borderline cases. For example, the tenrec and hedgehog appear to have "spikes" rather than hair. However, tenrec and hedgehog spikes (as well as porcupine quills), are modified hairs (Leon Augustus, 1920), so we classified tenrec and hedgehog as hairy. Armadillo, pig, and human are likewise classified as hairless species but have relatively greater hair quantity than the other hairless species. The armadillo, like the tenrec and hedgehog, has a unique external modification, but unlike the tenrec and hedgehog, the armadillo's shell is made of bone, not hair (I. H. Chen et al., 2011), so we classified the armadillo as hairless. Pig and human, on the other hand, have non-modified skin that is nearly completely covered in hair (and in the case of humans, the hair is quite dense in some body areas), but both species have large swaths of body area where hair is so sparse that sun-exposed skin is clearly visible. Both species were classified as hairless due to this pervasive low hair density. To assess the impact of species assignment on skin- and hair-related signal, hairless species were systematically removed and relevant enrichment statistics were recalculated. No specific species has a consistently detrimental impact on enrichment for gene sets of interest (Figure 4).

Calculating element-specific association statistics

For each genetic element, evolutionary rates for haired species versus hairless species were compared using Kendall's Tau. Haired species included ancestral species inferred to be haired in addition to extant haired species. Resulting p-values were multiple hypothesis testing corrected using a standard Benjamini-Hochberg correction (Benjamini & Hochberg, 1995).

In addition to calculating parametric p-values, empirical p-values were calculated using a novel permulation strategy modified from a similar strategy developed for continuous phenotypes (Kowalczyk et al., 2020). First, 1,000 null phenotypes were generated by using Brownian motion phylogenetic simulations and assigning the top ten values as hairless species. Resulting phenotypes were backpropagated along the phylogeny to ensure that final null phenotypes contained a total of eleven foreground species with only a single ancestral species classified as hairless. Such a procedure matched the organization of null phenotype values to true phenotype values. Hypothesis testing was repeating using all null phenotypes, and the

empirical p-values were calculated as the proportion of permulations with statistics as extreme or more extreme than the parametric statistic for the real phenotype values.

Calculating element-specific Bayes Factors

In addition to calculating element-specific association statistics, Bayes factors were calculated for each gene using the marine and hairless phenotypes. Briefly, Bayes factors quantify the support for a linear model predicting phenotype using evolutionary rate information from each gene, with a higher Bayes factor indicating greater support. The ratio of Bayes factors between the hairless and marine phenotypes quantifies the level of support of one phenotype over the other and thus can be used to tease apart intricacies of the two heavily-confounded phenotypes.

Calculating enrichment statistics

Enrichment statistics were calculated using Mouse Genome Informatics (MGI) gene sets (Blake et al., 2003), GTEx tissue annotations (Papatheodorou et al., 2018), GO annotations (Ashburner et al., 2000; Carbon et al., 2019), and genes highly expressed in hair follicles (Zhang et al., 2017). The 70 hair-follicle-specific genes were obtained by selecting the top 200 hair-follicle-expressed genes and removing genes that were included in the top 10,000 genes with the highest minimum median expression across GTEx tissues, i.e. ubiquitously expressed genes. Noncoding regions were mapped to annotations via distance from relevant genes – regions within 10,000 bases of a gene were assigned to that gene and its pathways. Noncoding regions were also mapped to microRNA coordinates using the same distance-based metric. All annotations are available at: https://pitt.box.com/s/b8ozkcwzile4znq8tw9ri8s160zjb3uw

Pathway enrichment statistics were calculated using the Wilcoxon Rank-Sum Test, which compares ranks of foreground values for elements in a pathway to background values for non-pathway elements. For each gene or noncoding element, the sign of the statistic times the log of the p-value were used to generate ranks. Empirical p-values from permulations were also generated using the same null phenotypes used for individual elements and detailed in previous work (Kowalczyk et al., 2020).

Permulations

In addition to computing parametric statistics directly from standard statistical tests, empirical p-values were also calculated using a permulation strategy. Permulations were used to generate null phenotype values, and the empirical p-value was calculated as the proportion of null statistics as extreme or more extreme than the observed parametric statistics. Such a strategy corrects for a non-uniform empirical null distribution at the gene level (Figure 1) and non-independence among genetic elements at the pathway level (Saputra et al., 2020).

Positive Selection Tests

For top-ranked genes under accelerated evolution in hairless species, all KRT and KRTAP genes, and various genes in top-ranked pathways under accelerated evolution in hairless species, branch-site models to test for positive selection were performed identify if rapidly-evolving genes were undergoing positive selection or merely under relaxation of constraint. Such models were performed using a subset of the full 62 species mammalian phylogeny as shown in the “Phylogenetic Trees” section below.

Significance of relaxation of constraint for hairless species was assessed using likelihood ratio tests (LRT) between Branch-site Neutral (BS Neutral) and its nested null model M1 (sites neutral model) in PAML (Yang, 2007). Similarly, LRTs between branch-site selection model (BS Alt Mod) and its null BS Neutral were used to infer positive selection in hairless species. For each test, p-values were estimated using the chi-square distribution with one degree of freedom. Phylogeny-wide relaxation of constraint was additionally quantified using the LRTs between M2 (sites selection model) vs M1 (sites neutral model) and M8 (sites selection model) vs M8A (sites neutral model) respectively. Prior to performing the mammal-wide tests, hairless foreground species were removed to allow for unbiased estimates of significance of relaxation of constraint and positive selection from only the background mammalian branches. Genes with significant signals of positive selection and non-significant signals of phylogeny-wide acceleration were inferred to be under positive selection.

Phylogenetic Trees

Master tree topology with average branch lengths:

((((((((((((ailMel1:0.03854019703,((lepWed1:0.02002160645,odoRosDi:0.02064385875):0.01734764946,musFur1:0.04613997497):0.002879093616):0.009005888384,canFam3:0.05339127565):0.01185166857,felCat5:0.05020331605):0.03285617057,((((((bosTau7:0.02168740723,((capHir1:0.01157093136,oviAri3:0.01246322594):0.0049716126,panHod1:0.01522587482):0.01465511149):0.0662523666,(orcOrc1:0.006371664911,turTru2:0.01086552617):0.06014682602):0.01216198069,susScr3:0.0796745271):0.006785823323,(camFer1:0.01240650215,vicPac2:0.01096629635):0.06374554586):0.02551888691,(cerSim1:0.04977357056,equCab2:0.061454379):0.02510111297):0.00331214686,((eptFus1:0.03248546656,(myoDav1:0.02344332842,myoLuc2:0.01567729315):0.02193849809):0.09455328094,(pteAle1:0.005833353548,pteVam1:0.01611220178):0.07567400302):0.02385546003):0.002057771224):0.004845253848,(conCri1:0.1239823369,(eriEur2:0.1696142244,sorAra2:0.1934205791):0.02079474546):0.0235875333):0.01477733374,((((((chrAsi1:0.1017903453,echTel2:0.1749615473):0.01592632003,eleEdw1:0.1516860647):0.006610995228,oryAfe1:0.08326528894):0.008243787904,(loxAfr3:0.06812658238,triMan1:0.06198982615):0.0224994529):0.03384011363,dasNov3:0.1342602666):0.005989703247,(((macEug2:0.1270943532,sarHar1:0.09944141622):0.02717055443,monDom5:0.1181200712):0.1802966572,ornAna1:0.4322118716):0.2206952867):0.01316436193):0.01425600689,((((((cavPor3:0.09048639907,(chiLan1:0.05332953299,octDeg1:0.08476954109):0.01287861561):0.02118937782,hetGla2:0.08588673524):0.07432515556,speTri2:0.08896424642):0.006291577528,(((criGri1:0.04084640027,mesAur1:0.04456203524):0.02314125062,micOch1:0.06932402649):0.01947113467,(mm10:0.05273642272,rn5:0.05576007402):0.04435347588):0.08380065137,jacJac1:0.1438649666):0.04270536633):0.01663675397,(ochPri3:0.1256544445,oryCun2:0.07131655591):0.06535533418):0.009050428462,tupChi1:0.1191189141):0.003894252213):0.01379370868,otoGar3:0.108738222):0.04299750653,(calJac3:0.02474184521,saiBol1:0.02096868307):0.02784675729):0.0135408115,(chlSab1:0.007693724903,((macFas5:0.001292320552,rheMac3:0.00713015786):0.002951690224,papHam1:0.005199240711):0.002049749893):0.01566263562):0.007043113559,nomLeu3:0.01770384793):0.002187630666,ponAbe2:0.0164503644):0.005572327638,gorGor3:0.007765177171):0.001382639829,hg19:0.005957477577,panTro4:0.006721826689);

Subset of master tree used for branch-site models for positive selection:

((((((((((lepWed1:0.02002160645,odoRosDi:0.02064385875):0.01734764946,musFur1:0.04613997497):0.02373665057,felCat5:0.05020331605):0.03285617057,((((((bosTau7:0.02168740723,oviAri3:0.03208995002):0.0662523666,(orcOrc1:0.006371664911,turTru2:0.01086552617):0.06014682602):0.01216198069,susScr3:0.0796745271):0.006785823323,vicPac2:0.0747118422):0.02551888691,(cerSim1:0.04977357056,equCab2:0.061454379):0.02510111297):0.00331214686,(myoDav1:0.1399351075,pteAle1:0.08150735657):0.02385546003):0.002057771224):0.004845253848,(conCri1:0.1239823369,sorAra2:0.2142153246):0.0235875333):0.01477733374,(((eleEdw1:0.1582970599,oryAfe1:0.08326528894):0.008243787904,(loxAfr3:0.06812658238,triMan1:0.06198982615):0.0224994529):0.03384011363,dasNov3:0.1342602666):0.01915406518):0.01425600689,(((((cavPor3:0.1116757769,hetGla2:0.08588673524):0.07432515556,speTri2:0.08896424642):0.006291577528,((criGri1:0.08345878555,mm10:0.09708989861):0.08380065137,jacJac1:0.1438649666):0.04270536633):0.01663675397,oryCun2:0.1366718901):0.009050428462,tupChi1:0.1191189141):0.003894252213):0.01379370868,otoGar3:0.108738222):0.04299750653,calJac3:0.0525886025):0.0135408115,(chlSab1:0.007693724903,rheMac3:0.012131597978):0.01566263562):0.01618571169,hg19:0.005957477577,panTro4:0.006721826689);

References

Ahmad, W., Ul Haque, M. F., Brancolini, V., Tsou, H. C., Ul Haque, S., Lam, H., … Christiano, A. M. (1998). Alopecia universalis associated with a mutation in the human hairless gene. *Science*, *279*(5351), 720–724. https://doi.org/10.1126/science.279.5351.720

Aldinger, K. A., Lehmann, O. J., Hudgins, L., Chizhikov, V. V, Bassuk, A. G., Ades, L. C., … Millen, K. J. (2009). FOXC1 is required for normal cerebellar development and is a major contributor to chromosome 6p25.3 Dandy-Walker malformation. *Nature Genetics*, *41*(9), 1037–1042. https://doi.org/10.1038/ng.422

Alonso, L., & Fuchs, E. (2006). The hair cycle. *Journal of Cell Science*, *119*(3), 391–393. https://doi.org/10.1242/jcs.02793

Andl, T., & Botchkareva, N. V. (2015). MicroRNAs (miRNAs) in the control of HF development and cycling: The next frontiers in hair research. *Experimental Dermatology*, *24*(11), 821–826. https://doi.org/10.1111/exd.12785

Ashburner, M., Ball, C. A., Blake, J. A., Botstein, D., Butler, H., Cherry, J. M., … Sherlock, G. (2000, May). Gene ontology: Tool for the unification of biology. *Nature Genetics*, Vol. 25, pp. 25–29. https://doi.org/10.1038/75556

Aya, U. I., Shimokawa, I., & Doi, K. (2009). Time-course expression profiles of hair cycle-associated genes in male mini rats after depilation of telogen-phase hairs. *International Journal of Molecular Sciences*, *10*(5), 1967–1977. https://doi.org/10.3390/ijms10051967

Benavides, F., Oberyszyn, T. M., VanBuskirk, A. M., Reeve, V. E., & Kusewitt, D. F. (2009, January 1). The hairless mouse in skin research. *Journal of Dermatological Science*, Vol. 53, pp. 10–18. https://doi.org/10.1016/j.jdermsci.2008.08.012

Benjamini, Y., & Hochberg, Y. (1995). Controlling the False Discovery Rate: A Practical and Powerful Approach to Multiple. In *Source: Journal of the Royal Statistical Society. Series B (Methodological)* (Vol. 57). Retrieved from https://www-jstor-org.pitt.idm.oclc.org/stable/pdf/2346101.pdf?refreqid=excelsior%3A56a1f0a45f63fb9afb0267135a742b13

Blake, J. A., Richardson, J. E., Bult, C. J., Kadin, J. A., Eppig, J. T., & Mouse Genome Database Group. (2003). MGD: the Mouse Genome Database. *Nucleic Acids Research*, *31*(1), 193–

195. Retrieved from http://www.ncbi.nlm.nih.gov/pubmed/12519980

Blanchette, M., Kent, W. J., Riemer, C., Elnitski, L., Smit, A. F. A., Roskin, K. M., … Miller, W. (2004). Aligning multiple genomic sequences with the threaded blockset aligner. *Genome Research*, *14*(4), 708–715. https://doi.org/10.1101/gr.1933104

Blumenberg, M. (2013). *Transcriptional Regulation of Keratin Gene Expression*. Retrieved from https://www.ncbi.nlm.nih.gov/books/NBK6213/

Brembeck, F. H., Opitz, O. G., Libermann, T. A., & Rustgi, A. K. (2000). Dual function of the epithelial specific ets transcription factor, ELF3, in modulating differentiation. *Oncogene*, *19*(15), 1941–1949. https://doi.org/10.1038/sj.onc.1203441

Callister, R. J. (2010). Early history of glycine receptor biology in mammalian spinal cord circuits. *Frontiers in Molecular Neuroscience*, *3*, 13. https://doi.org/10.3389/fnmol.2010.00013

Carbon, S., Douglass, E., Dunn, N., Good, B., Harris, N. L., Lewis, S. E., … Westerfield, M. (2019). The Gene Ontology Resource: 20 years and still GOing strong. *Nucleic Acids Research*, *47*(D1), D330–D338. https://doi.org/10.1093/nar/gky1055

Carrasco, E., Calvo, M. I., Blázquez-Castro, A., Vecchio, D., Zamarrón, A., De Almeida, I. J. D., … Espada, J. (2015). Photoactivation of ROS Production in Situ Transiently Activates Cell Proliferation in Mouse Skin and in the Hair Follicle Stem Cell Niche Promoting Hair Growth and Wound Healing. *Journal of Investigative Dermatology*, *135*(11), 2611–2622. https://doi.org/10.1038/jid.2015.248

Chen, I. H., Kiang, J. H., Correa, V., Lopez, M. I., Chen, P. Y., McKittrick, J., & Meyers, M. A. (2011). Armadillo armor: Mechanical testing and micro-structural evaluation. *Journal of the Mechanical Behavior of Biomedical Materials*, *4*(5), 713–722. https://doi.org/10.1016/j.jmbbm.2010.12.013

Chen, Z., Wang, Z., Xu, S., Zhou, K., & Yang, G. (2013). Characterization of hairless (Hr) and FGF5 genes provides insights into the molecular basis of hair loss in cetaceans. *BMC Evolutionary Biology*, *13*(1), 1–11. https://doi.org/10.1186/1471-2148-13-34

Chikina, M., Robinson, J. D., & Clark, N. L. (2016). Hundreds of Genes Experienced Convergent Shifts in Selective Pressure in Marine Mammals. *Molecular Biology and Evolution*, *33*(9), 2182–2192. https://doi.org/10.1093/molbev/msw112

Cui, Y., Song, Y., Geng, Q., Ding, Z., Qin, Y., Fan, R., … Geng, J. (2016). The expression of KRT2 and its effect on melanogenesis in alpaca skins. *Acta Histochemica*, *118*(5), 505–512. https://doi.org/10.1016/j.acthis.2016.05.004

Donet, E., Bayo, P., Calvo, E., Labrie, F., & Pérez, P. (2008). Identification of novel glucocorticoid receptor-regulated genes involved in epidermal homeostasis and hair follicle differentiation. *Journal of Steroid Biochemistry and Molecular Biology*, *108*(1–2), 8–16. https://doi.org/10.1016/j.jsbmb.2007.05.033

Drögemüller, C., Karlsson, E. K., Hytönen, M. K., Perloski, M., Dolf, G., Sainio, K., … Leeb, T. (2008). A mutation in hairless dogs implicates FOXI3 in ectodermal development. *Science*, *321*(5895), 1462. https://doi.org/10.1126/science.1162525

Eckhart, L., Dalla Valle, L., Jaeger, K., Ballaun, C., Szabo, S., Nardi, A., … Tschachler, E. (2008). *Identification of reptilian genes encoding hair keratin-like proteins suggests a new scenario for the evolutionary origin of hair*. Retrieved from www.pnas.orgcgidoi10.1073pnas.0805154105

Edgar, R. C. (2004). MUSCLE: Multiple sequence alignment with high accuracy and high throughput. *Nucleic Acids Research*, *32*(5), 1792–1797. https://doi.org/10.1093/nar/gkh340

Eppig, J. T., Blake, J. A., Bult, C. J., Kadin, J. A., Richardson, J. E., & Mouse Genome Database Group, T. M. G. D. (2015). The Mouse Genome Database (MGD): facilitating mouse as a model for human biology and disease. *Nucleic Acids Research*, *43*(Database issue), D726-36. https://doi.org/10.1093/nar/gku967

Fu, S., Zhao, H., Zheng, Z., Li, J., & Zhang, W. (2014). Melatonin regulating the expression of miRNAs involved in hair follicle cycle of cashmere goats skin. *Yi Chuan = Hereditas / Zhongguo Yi Chuan Xue Hui Bian Ji*, *36*(12), 1235–1242. https://doi.org/10.3724/SP.J.1005.2014.1235

Fuller, A., Mitchell, D., Maloney, S. K., & Hetem, R. S. (2016). Towards a mechanistic understanding of the responses of large terrestrial mammals to heat and aridity associated with climate change. *Climate Change Responses*, *3*(1), 1–19. https://doi.org/10.1186/s40665-016-0024-1

Harris, R. S. (2007). *Improved Pairwise Alignment of Genomic DNA*. Retrieved from https://etda.libraries.psu.edu/catalog/7971

Heitman, N., Sennett, R., Mok, K. W., Saxena, N., Srivastava, D., Martino, P., … Rendl, M. (2020). Dermal sheath contraction powers stem cell niche relocation during hair cycle regression. *Science*, *367*(6474), 161–166. https://doi.org/10.1126/science.aax9131

Hiller, M., Schaar, B. T., Indjeian, V. B., Kingsley, D. M., Hagey, L. R., & Bejerano, G. (2012). A "Forward Genomics" Approach Links Genotype to Phenotype using Independent Phenotypic Losses among Related Species. *Cell Reports*, *2*(4), 817–823. https://doi.org/10.1016/J.CELREP.2012.08.032

Hofmann, S., Franke, A., Fischer, A., Jacobs, G., Nothnagel, M., Gaede, K. I., … Schreiber, S. (2008). *Genome-wide association study identifies ANXA11 as a new susceptibility locus for sarcoidosis*. https://doi.org/10.1038/ng.198

Hu, Z., Sackton, T. B., Edwards, S. V., & Liu, J. S. (2019). Bayesian Detection of Convergent Rate Changes of Conserved Noncoding Elements on Phylogenetic Trees. *Molecular Biology and Evolution*, *36*(5), 1086–1100. https://doi.org/10.1093/molbev/msz049

Jahoda, C. A.B., Horne, K. A., & Oliver, R. F. (1984). Induction of hair growth by implantation of cultured dermal papilla cells. *Nature*, *311*(5986), 560–562. https://doi.org/10.1038/311560a0

Jahoda, Colin A.B., Reynolds, A. J., & Oliver, R. F. (1993). Induction of hair growth in ear wounds by cultured dermal papilla cells. *Journal of Investigative Dermatology*, *101*(4), 584–590. https://doi.org/10.1111/1523-1747.ep12366039

Jaks, V., Barker, N., Kasper, M., Van Es, J. H., Snippert, H. J., Clevers, H., & Toftgård, R. (2008). Lgr5 marks cycling, yet long-lived, hair follicle stem cells. *Nature Genetics*, *40*(11), 1291–1299. https://doi.org/10.1038/ng.239

Johnson, E. (1981). Environmental Influences on the Hair Follicle. In *Hair Research* (pp. 183–194). https://doi.org/10.1007/978-3-642-81650-5_27

Kapheim, K. M., Pan, H., Li, C., Salzberg, S. L., Puiu, D., Magoc, T., … Zhang, G. (2015). Genomic signatures of evolutionary transitions from solitary to group living. *Science*, *348*(6239), 25. https://doi.org/10.1126/science.aaa4788

Kawano, M., Komi-Kuramochi, A., Asada, M., Suzuki, M., Oki, J., Jiang, J., & Imamura, T. (2005). Comprehensive analysis of FGF and FGFR expression in skin: FGF18 is highly expressed in hair follicles and capable of inducing anagen from telogen stage hair follicles. *Journal of Investigative Dermatology*, *124*(5), 877–885. https://doi.org/10.1111/j.0022-202X.2005.23693.x

Kent, W. J., Sugnet, C. W., Furey, T. S., Roskin, K. M., Pringle, T. H., Zahler, A. M., & Haussler, D. (2002). The human genome browser at UCSC. *Genome Research*, *12*(6), 996–1006. https://doi.org/10.1101/gr.229102

Kettunen, P., Furmanek, T., Chaulagain, R., Hals Kvinnsland, I., & Luukko, K. (2011). Developmentally regulated expression of intracellular Fgf11-13, hormone-like Fgf15 and canonical Fgf16, -17 and -20 mRNAs in the developing mouse molar tooth. *Acta Odontologica Scandinavica*, *69*(6), 360–366. https://doi.org/10.3109/00016357.2011.568968

Kowalczyk, A., Meyer, W., Partha, R., Mao, W., Clark, N., & Chikina, M. (2019). RERconverge: an R package for associating evolutionary rates with convergent traits. *Bioinformatics*, *35*(22), 4815–4817. https://doi.org/10.1101/451138

Kowalczyk, A., Partha, R., Clark, N. L., & Chikina, M. (2020). Pan-mammalian analysis of molecular constraints underlying extended lifespan. *ELife*, *9*. https://doi.org/10.7554/eLife.51089

Kushlan, J. A. (1980). The Evolution of Hairlessness in Man. *The American Naturalist*, *116*(5), 727–729. https://doi.org/10.1086/283663

Lay, K., Kume, T., & Fuchs, E. (2016). FOXC1 maintains the hair follicle stem cell niche and governs stem cell quiescence to preserve long-term tissue-regenerating potential. *Proceedings of the National Academy of Sciences of the United States of America*, *113*(11), E1506–E1515. https://doi.org/10.1073/pnas.1601569113

Lee, K. H., Choi, D., Jeong, S. Il, Kim, S. J., Lee, C. H., Seo, H. S., & Jeong, H. S. (2019). Eclipta prostrata promotes the induction of anagen, sustains the anagen phase through regulation of FGF-7 and FGF-5. *Pharmaceutical Biology*, *57*(1), 105–111. https://doi.org/10.1080/13880209.2018.1561729

Leon Augustus, H. (1920). Structural Characteristics of the Hair of Mammals. *The American Naturalist*, *54*(635), 496–523. https://doi.org/10.2307/2456345

Li, G., Zhou, S., Li, C., Cai, B., Yu, H., Ma, B., … Wang, X. (2019). Base pair editing in goat: nonsense codon introgression into FGF5 results in longer hair. *FEBS Journal*, *286*(23), 4675–4692. https://doi.org/10.1111/febs.14983

Liang, P., Lv, C., Jiang, B., Long, X., Zhang, P., Zhang, M., … Huang, X. (2012). MicroRNA profiling in denatured dermis of deep burn patients. *Burns*, *38*(4), 534–540. https://doi.org/10.1016/j.burns.2011.10.014

Liberzon, A., Subramanian, A., Pinchback, R., Thorvaldsdóttir, H., Tamayo, P., & Mesirov, J. P. (2011). Molecular signatures database (MSigDB) 3.0. *Bioinformatics (Oxford, England)*, *27*(12), 1739–1740. https://doi.org/10.1093/bioinformatics/btr260

Lin, Z., Chen, Q., Shi, L., Lee, M., Giehl, K. A., Tang, Z., … Yang, Y. (2012). Loss-of-function mutations in HOXC13 cause pure hair and nail ectodermal dysplasia. *American Journal of Human Genetics*, *91*(5), 906–911. https://doi.org/10.1016/j.ajhg.2012.08.029

Mesler, A. L., Veniaminova, N. A., Lull, M. V., & Wong, S. Y. (2017). Hair Follicle Terminal Differentiation Is Orchestrated by Distinct Early and Late Matrix Progenitors. *Cell Reports*, *19*(4), 809–821. https://doi.org/10.1016/j.celrep.2017.03.077

Meyer, W. K., Jamison, J., Richter, R., Woods, S. E., Partha, R., Kowalczyk, A., … Clark, N. L. (2018). Ancient convergent losses of Paraoxonase 1 yield potential risks for modern marine mammals. *Science (New York, N.Y.)*, *361*(6402), 591–594. https://doi.org/10.1126/science.aap7714

Michel, L., Reygagne, P., Benech, P., Jean-Louis, F., Scalvino, S., Ly Ka So, S., … Hocquaux,

M. (2017). Study of gene expression alteration in male androgenetic alopecia: evidence of predominant molecular signalling pathways. *British Journal of Dermatology*, *177*(5), 1322–1336. https://doi.org/10.1111/bjd.15577

Muñoz, J., Stange, D. E., Schepers, A. G., Van De Wetering, M., Koo, B. K., Itzkovitz, S., … Clevers, H. (2012). The Lgr5 intestinal stem cell signature: Robust expression of proposed quiescent ′ +4′ cell markers. *EMBO Journal*, *31*(14), 3079–3091. https://doi.org/10.1038/emboj.2012.166

Nagao, K., Kobayashi, T., Moro, K., Ohyama, M., Adachi, T., Kitashima, D. Y., … Amagai, M. (2012). Stress-induced production of chemokines by hair follicles regulates the trafficking of dendritic cells in skin. *Nature Immunology*, *13*(8), 744–752. https://doi.org/10.1038/ni.2353

Nakatake, Y., Hoshikawa, M., Asaki, T., Kassai, Y., & Itoh, N. (2001). Identification of a novel fibroblast growth factor, FGF-22, preferentially expressed in the inner root sheath of the hair follicle. *Biochimica et Biophysica Acta - Gene Structure and Expression*, *1517*(3), 460–463. https://doi.org/10.1016/S0167-4781(00)00302-X

Nery, M. F., Arroyo, J. I., & Opazo, J. C. (2014). Increased rate of hair keratin gene loss in the cetacean lineage. *BMC Genomics*, *15*(1), 1–9. https://doi.org/10.1186/1471-2164-15-869

Papatheodorou, I., Fonseca, N. A., Keays, M., Tang, Y. A., Barrera, E., Bazant, W., … Petryszak, R. (2018). Expression Atlas: Gene and protein expression across multiple studies and organisms. *Nucleic Acids Research*, *46*(D1), D246–D251. https://doi.org/10.1093/nar/gkx1158

Parker, H. G., Harris, A., Dreger, D. L., Davis, B. W., & Ostrander, E. A. (2017). The bald and the beautiful: hairlessness in domestic dog breeds. *Philosophical Transactions of the Royal Society B: Biological Sciences*, *372*(1713), 20150488. https://doi.org/10.1098/rstb.2015.0488

Partha, R., Chauhan, B. K., Ferreira, Z., Robinson, J. D., Lathrop, K., Nischal, K. K., … Clark, N. L. (2017). Subterranean mammals show convergent regression in ocular genes and enhancers, along with adaptation to tunneling. *ELife*, *6*. https://doi.org/10.7554/eLife.25884

Partha, R., Kowalczyk, A., Clark, N. L., & Chikina, M. (2019). Robust method for detecting convergent shifts in evolutionary rates. *Molecular Biology and Evolution*, *36*(8), 1817–1830. https://doi.org/10.1101/457309

Peng, H., Park, J. K., Katsnelson, J., Kaplan, N., Yang, W., Getsios, S., & Lavker, R. M. (2015). microRNA-103/107 Family Regulates Multiple Epithelial Stem Cell Characteristics. *STEM CELLS*, *33*(5), 1642–1656. https://doi.org/10.1002/STEM.1962@10.1002/(ISSN)1549-4918.THEBESTPAPERSFROMOUR2016YOUNGINVESTIGATORS

Plowman, J., Harland, D., & Deb-Choudhury, S. (2018). *The Hair Fibre: Proteins, Structure and Development* (I. Cohen, A. Lajtha, J. Lambris, R. Paoletti, & N. Rezaei, Eds.). Singapore.

Pough, F., Heiser, J., & McFarland, W. (1989). *Vertebrate Life*. New York: Macmillan Publishing Company.

Prudent, X., Parra, G., Schwede, P., Roscito, J. G., & Hiller, M. (2016). Controlling for Phylogenetic Relatedness and Evolutionary Rates Improves the Discovery of Associations Between Species' Phenotypic and Genomic Differences. *Molecular Biology and Evolution*, *33*(8), 2135–2150. https://doi.org/10.1093/molbev/msw098

Reynolds, A. J., & Jahoda, C. A. (1992). Cultured dermal papilla cells induce follicle formation and hair growth by transdifferentiation of an adult epidermis. *Development*, *115*(2).

Rezza, A., Wang, Z., Sennett, R., Qiao, W., Wang, D., Heitman, N., … Rendl, M. (2016).

Signaling Networks among Stem Cell Precursors, Transit-Amplifying Progenitors, and their Niche in Developing Hair Follicles. *Cell Reports*, *14*(12), 3001–3018. https://doi.org/10.1016/j.celrep.2016.02.078

Roca, A. L., Ishida, Y., Nikolaidis, N., Kolokotronis, S. O., Fratpietro, S., Stewardson, K., … Greenwood, A. D. (2009). Genetic variation at hair length candidate genes in elephants and the extinct woolly mammoth. *BMC Evolutionary Biology*, *9*(1), 232. https://doi.org/10.1186/1471-2148-9-232

Rosenquist, T. A., & Martin, G. R. (1996). Fibroblast growth factor signalling in the hair growth cycle: expression of the fibroblast growth factor receptor and ligand genes in the murine hair follicle. *Developmental Dynamics : An Official Publication of the American Association of Anatomists*, *205*(4), 379–386. https://doi.org/10.1002/(SICI)1097-0177(199604)205:4<379::AID-AJA2>3.0.CO;2-F

Santos, A., Tsafou, K., Stolte, C., Pletscher-Frankild, S., O'Donoghue, S. I., & Jensen, L. J. (2015). Comprehensive comparison of large-scale tissue expression datasets. *PeerJ*, *2015*(6). https://doi.org/10.7717/peerj.1054

Saputra, E., Kowalczyk, A., Cusick, L., Clark, N., & Chikina, M. (2020). Phylogenetic Permulations: a statistically rigorous approach to measure confidence in associations between phenotypes and genetic elements in a phylogenetic context. *BioRxiv*, 2020.10.14.338608. https://doi.org/10.1101/2020.10.14.338608

Sarasin, A. (2012). UVSSA and USP7: New players regulating transcription-coupled nucleotide excision repair in human cells. *Genome Medicine*, *4*(5), 44. https://doi.org/10.1186/gm343

Sengez, B., Aygün, I., Shehwana, H., Toyran, N., Tercan Avci, S., Konu, O., … Alotaibi, H. (2019). The Transcription Factor Elf3 Is Essential for a Successful Mesenchymal to Epithelial Transition. *Cells*, *8*(8), 858. https://doi.org/10.3390/cells8080858

Seo, S., Fujita, H., Nakano, A., Kang, M., Duarte, A., & Kume, T. (2006). The forkhead transcription factors, Foxc1 and Foxc2, are required for arterial specification and lymphatic sprouting during vascular development. *Developmental Biology*, *294*(2), 458–470. https://doi.org/10.1016/j.ydbio.2006.03.035

Siepel, A., Bejerano, G., Pedersen, J. S., Hinrichs, A. S., Hou, M., Rosenbloom, K., … Haussler, D. (2005). Evolutionarily conserved elements in vertebrate, insect, worm, and yeast genomes. *Genome Research*, *15*(8), 1034–1050. https://doi.org/10.1101/gr.3715005

Sprecher, E., Molho-Pessach, V., Ingber, A., Sagi, E., Indelman, M., & Bergman, R. (2004). Homozygous splice site mutations in PKP1 result in loss of epidermal plakophilin 1 expression and underlie ectodermal dysplasia/skin fragility syndrome in two consanguineous families. *Journal of Investigative Dermatology*, *122*(3), 647–651. https://doi.org/10.1111/j.0022-202X.2004.22335.x

Suárez-Fariñas, M., Ungar, B., Noda, S., Shroff, A., Mansouri, Y., Fuentes-Duculan, J., … Guttman-Yassky, E. (2015). Alopecia areata profiling shows TH1, TH2, and IL-23 cytokine activation without parallel TH17/TH22 skewing. *Journal of Allergy and Clinical Immunology*, *136*(5), 1277–1287. https://doi.org/10.1016/j.jaci.2015.06.032

Suzuki, S., Ota, Y., Ozawa, K., & Imamura, T. (2000). Dual-mode regulation of hair growth cycle by two Fgf-5 gene products. *Journal of Investigative Dermatology*, *114*(3), 456–463. https://doi.org/10.1046/j.1523-1747.2000.00912.x

Tacutu, R., Thornton, D., Johnson, E., Budovsky, A., Barardo, D., Craig, T., … de Magalhães, J. P. (2018). Human Ageing Genomic Resources: new and updated databases. *Nucleic Acids Research*, *46*(D1), D1083–D1090. https://doi.org/10.1093/nar/gkx1042

Veraitch, O., Mabuchi, Y., Matsuzaki, Y., Sasaki, T., Okuno, H., Tsukashima, A., … Ohyama, M. (2017). Induction of hair follicle dermal papilla cell properties in human induced pluripotent stem cell-derived multipotent LNGFR(+)THY-1(+) mesenchymal cells. *Scientific Reports*, *7*(1), 1–13. https://doi.org/10.1038/srep42777

Wang, D., Zhang, Z., O'Loughlin, E., Wang, L., Fan, X., Lai, E. C., & Yi, R. (2013). MicroRNA-205 controls neonatal expansion of skin stem cells by modulating the PI(3)K pathway. *Nature Cell Biology*, *15*(10), 1153–1163. https://doi.org/10.1038/ncb2827

Wang, L., Siegenthaler, J. A., Dowell, R. D., & Yi, R. (2016). Stem cells: Foxc1 reinforces quiescence in self-renewing hair follicle stem cells. *Science*, *351*(6273), 613–617. https://doi.org/10.1126/science.aad5440

Wertheim, J. O., Murrell, B., Smith, M. D., Kosakovsky Pond, S. L., & Scheffler, K. (2015). RELAX: Detecting Relaxed Selection in a Phylogenetic Framework. *Molecular Biology and Evolution*, *32*(3), 820–832. https://doi.org/10.1093/molbev/msu400

Xu, H. L., Chen, P. P., Wang, L. fen, Xue, W., & Fu, T. L. (2018). Hair regenerative effect of silk fibroin hydrogel with incorporation of FGF-2-liposome and its potential mechanism in mice with testosterone-induced alopecia areata. *Journal of Drug Delivery Science and Technology*, *48*, 128–136. https://doi.org/10.1016/j.jddst.2018.09.006

Yang, Z. (2007). PAML 4: Phylogenetic Analysis by Maximum Likelihood. *Molecular Biology and Evolution*, *24*(8), 1586–1591. https://doi.org/10.1093/molbev/msm088

Ye, S. B., Zhang, H., Cai, T. T., Liu, Y. N., Ni, J. J., He, J., … Li, J. (2016). Exosomal miR-24-3p impedes T-cell function by targeting FGF11 and serves as a potential prognostic biomarker for nasopharyngeal carcinoma. *Journal of Pathology*, *240*(3), 329–340. https://doi.org/10.1002/path.4781

Zerbino, D. R., Wilder, S. P., Johnson, N., Juettemann, T., & Flicek, P. R. (2015). The Ensembl Regulatory Build. *Genome Biology*, *16*(1). https://doi.org/10.1186/s13059-015-0621-5

Zhang, J., Wallace, S. J., Shiu, M. Y., Smith, I., Rhind, S. G., & Langlois, V. S. (2017). Human hair follicle transcriptome profiling: A minimally invasive tool to assess molecular adaptations upon low-volume, high-intensity interval training. *Physiological Reports*, *5*(23), e13534. https://doi.org/10.14814/phy2.13534

Zhou, L., Wang, H., Jing, J., Yu, L., Wu, X., & Lu, Z. (2018). Regulation of hair follicle development by exosomes derived from dermal papilla cells. *Biochemical and Biophysical Research Communications*, *500*(2), 325–332. https://doi.org/10.1016/j.bbrc.2018.04.067